arXiv:2202.11912v1 [cs.LG] 24 Feb 2022

A RIGOROUS STUDY OF INTEGRATED GRADIENTS METHOD AND EXTENSIONS TO INTERNAL NEURON ATTRIBUTIONS

Daniel Lundstrom
Department of Mathematics
University of Southern California
California, CA 90089
lundstro@usc.edu

Tianjian Huang
Department of Industrial & System Engineering
University of Southern California
California, CA 90089
tianjian@usc.edu

Meisam Razaviyayn
Department of Industrial & System Engineering
University of Southern California
California, CA 90089
razaviya@usc.edu

ABSTRACT

As the efficacy of deep learning (DL) grows, so do concerns about the lack of transparency of these black-box models. Attribution methods aim to improve transparency of DL models by quantifying an input feature's importance to a model's prediction. The method of Integrated gradients (IG) sets itself apart by claiming other methods failed to satisfy desirable axioms, while IG and methods like it uniquely satisfied said axioms. This paper comments on fundamental aspects of IG and its applications/extensions: 1) We identify key unaddressed differences between DL-attribution function spaces and the supporting literature's function spaces which problematize previous claims of IG uniqueness. We show that with the introduction of an additional axiom, *non-decreasing positivity*, the uniqueness claim can be established. 2) We address the question of input sensitivity by identifying function spaces where the IG is/is not Lipschitz continuous in the attributed input. 3) We show how axioms for single-baseline methods in IG impart analogous properties for methods where the baseline is a probability distribution over the input sample space. 4) We introduce a means of decomposing the IG map with respect to a layer of internal neurons while simultaneously gaining internal-neuron attributions. Finally, we present experimental results validating the decomposition and internal neuron attributions.

1 Introduction

Deep neural networks have revolutionized the field of vision processing, showing marked accuracy for varied and large scale computer vision tasks [Huang et al., 2017], [Ren et al., 2016], [Bochkovskiy et al., 2020]. At the same time, deep neural networks suffer from a lack of interpretability. Various methods have been developed to address the interpretability problem by quantifying, or attributing, the importance of each input feature to a model's output. Basic techniques inspect the gradient of the output with respect to an input [Baehrens et al., 2010]. Deconvolutional networks [Zeiler and Fergus, 2014] employ deep networks to produce attributions, while guided back-propagation [Springenberg et al., 2014] gives attributions to internal neuron activation. Methods such as Deeplift [Shrikumar et al., 2017] and Layer-wise relevance propagation [Binder et al., 2016] employ a baseline to use as a comparison to the input (called baseline attributions). Further methods include Zhou et al. [2016], Zintgraf et al. [2016].

Sundararajan et al. [2017] introduced the baseline attribution method of Integrated Gradients (IG) and identified the method's advantages. The paper identified a set of desirable axioms for attributions, demonstrated that previous methods fail to satisfy them, and introduced the IG method which satisfied the axioms. Included was a claim that any method

that satisfied a subset of the axioms must be a more general form of IG (called path methods). A noteworthy extension to IG appears in Erion et al. [2021], where the average IG over a distribution of baselines is considered.

Contributions. This paper addressed multiple aspects of the IG method: its foundational claims, mathematical behavior, and extensions. The IG paper of Sundararajan et al. [2017] applies results from Friedman [2004] (given here as Theorem 1) to claim that path methods (defined below) are the only methods that satisfy a set of desirable axioms. Upon inspection, we observed that there are key assumptions of the function spaces of Friedman [2004], such as functions being non-decreasing, which are not true in the DL context. These differences in function spaces were unaddressed in Sundararajan et al. [2017]. We show that because the function spaces differ, Theorem 1 does not apply and the uniqueness claim is false. With the introduction of an additional axiom, *non-decreasing positivity* (NDP), we show that Theorem 1 can apply, and rigorously extend it into a basic DL function space.

We address the mathematical behavior of IG and an extension. We identify a common class of functions where IG may be hypersensitive to the input image by failing to be Lipschitz continuous, as well as a function class where IG is guaranteed to be Lipschitz continuous. We also observe that the axioms in Sundararajan et al. [2017] apply to single baseline attribution methods. No such axioms have been stated for methods that employ a distribution of baselines. We identify/extend axioms for the distribution of baselines methods that parallel those in the single baseline case.

Lastly, we introduce a means of decomposing the IG attribution map by a layer of internal neurons. This produces attribution sub-maps for each neuron which, summed together, equal the original IG map. Additionally, each sub-map yields an attribution score for the neuron. This allows one to inspect if individual neurons are responsible for a particular feature or region of the IG map. Our decomposition can be used to identify which neurons are associated with identifying particular categories. We demonstrate the practicality of the method with experiments on fashion MNIST.

2 Background

2.1 Attribution Methods and Integrated Gradient

For $a, b \in \mathbb{R}^n$, define $[a, b]$ to be the hyperrectangle with a, b as opposite vertices. An example is a greyscale image, which would have $a = 0, b$ be the vectorized pixel values of a white image, and n be the pixel count. We denote a class of functions $F : [a, b] \to \mathbb{R}$ by $\mathcal{F}(a, b)$, or $\mathcal{F}$ if a, b may be inferred from the context. An example is a DL object recognition model classifying images in a classification task. A *baseline attribution method* (BAM) is defined as follows:

Definition 1 (Baseline Attribution Method)**.** [1] Given $x, x' \in [a, b]$, $F \in \mathcal{F}(a, b)$, a baseline attribution method is any function of the form $A : [a, b] \times [a, b] \times \mathcal{F}(a, b) \to \mathbb{R}^n$.

We may drop x' and write $A(x, F)$ if the baseline is fixed, or may be inferred. An attribution can be interpreted as assigning values to each input x_i indicating x_i's contribution to the model output, $F(x)$. Obviously, many BAMs in the function class do not practically track an input's contribution to an output. By considering properties desirable to an attribution method, we may restrict the function space further to those which more effectively track input contributions. To this end, let us define a *path function* as follows:

Definition 2 (Path Function)**.** A function $\gamma(x, x', t) : [a, b] \times [a, b] \times [0, 1] \to [a, b]$ is a path function if, for fixed x, x', $\gamma(t) := \gamma(x, x', t)$ is a continuous, piecewise smooth curve from x' to x.

We may drop x' or both x, x' when they are fixed, and write $\gamma(x, t)$, $\gamma(t)$ respectively. If we further suppose that $\frac{\partial F}{\partial x_i}(\gamma(t))$ exists almost everywhere[2], then the *path method* associated with γ can be defined as:

Definition 3 (path method)**.** Given the path function $\gamma(\cdot, \cdot, \cdot)$, the corresponding path method is defined as

$$A^\gamma(x, x', F) = \int_0^1 \frac{\partial F}{\partial x_i}(\gamma(x, x', t)) \times \frac{\partial \gamma_i}{\partial t}(x, x', t)dt, \tag{1}$$

where γ_i denotes the i-th entry of γ.

By definition, all path methods are baseline attribution methods. A *monotone path method* is a path attribution where each path is monotone, i.e., $\gamma_i(t)$ is monotone in t for all i.

The *integrated gradient* method is a path method where the path is a straight line from x to x'. Formally, choosing the monotone path $\gamma(t) = x' + t(x - x')$ yields the IG formula:

[1] It is possible to widen the definition of baseline attribution methods to include the model's implementation, not just the input and output. We use our definition for the scope of the paper.

[2] A function exists almost everywhere if the set of points where the function is not defined has Lebesgue measure 0.

Definition 4 (Integrated Gradient Method)**.** [3]Given $x, x' \in [a, b]$, and $F \in \mathcal{F}(a, b)$, the integrated gradient attribution of the i-th component of x is defined as

$$\text{IG}_i(x, x', F) = (x_i - x'_i) \int_0^1 \frac{\partial F}{\partial x_i}(x' + t(x - x'))dt \tag{2}$$

Sundararajan et al. [2017] uses a black baseline, i.e., $x' = 0$. IG corresponds to the Aumann-Shaply method in the cost sharing literature Aumann and Shapley [1974].

2.2 What makes IG unique?

The theoretical allure of IG stems from three key claims: 1) IG satisfied stipulated axioms (desirable properties), 2) other methods failed at least one of the axioms, and 3) only methods like it (path methods) were able to satisfy these axioms. Let us review the stated axioms in Sundararajan et al. [2017]. Let A be a BAM, $x, x' \in [a, b]$, $F, G \in \mathcal{F}$. Then the axioms are as follows:

1. *Sensitivity(a)*: Suppose x, x' vary in one component, so that $x_i \neq x'_i$, and $x_j = x'_j \; \forall j \neq i$. Further suppose $F(x) \neq F(x')$. Then $A_i(x, x', F) \neq 0$.
2. *Implementation Invariance*: A is not a function of model implementation, but solely of the mathematical mapping of the model's domain to the range.
3. *Completeness*: $\forall F \in \mathcal{F}$, $x, x' \in [a, b]$, we have: $\sum_{i=1}^{n} A_i(x, x', F) = F(x) - F(x')$.
4. *Linearity*: For $\alpha, \beta \in \mathbb{R}$, we have: $A_i(x, x', \alpha F + \beta G) = \alpha A_i(x, x', F) + \beta A_i(x, x', G)$.
5. *Sensitivity(b)/Dummy*: $\forall F \in \mathcal{F}$, if $\partial_i F \equiv 0$, then, $A_i(x, x', F) = 0$.
6. *Symmetry Preserving*: For a given (i, j), define x^* by swapping the values of x_i and x_j. Now suppose that $\forall x \in [a, b]$, $F(x) = F(x^*)$. Then whenever $x_i = x_j$ and $x'_i = x'_j$, we have $A_i(x, x', F) = A_j(x, x', F)$.

Here we give an explanation of each axiom. 1) Sensitivity(a) stipulates that if altering a baseline by a single input yields a different output, then that input should have some attribution score. 2) Implementation Invariance states that an attribution method should depend on the form of the function alone, not by any particular way it is coded up. In our formulation, this is a given, but it is possible to consider attribution methods that are a function of model implementation. 3) Completeness states that the sum of the attributions equals the change in function value. It allows an interpretation of each attribution as a contribution to a portion of the function value change. It does this by ensuring that the attribution function has a complete accounting of said change. 4) Linearity would be desirable in ensemble voting models, and indicates that the attribution to an input is the weighted sum of its attributions for the individual models, with the weights equal to the ensemble weights. 5) Sensitivity(b) is called dummy or dummy-consistency in Friedman [2004], and simply means that if an input does not affect the output, then it should have zero attribution. 6) Symmetry Preservation indicates that if two variables are universally interchangeable in the function, and their values are identical in the input and baseline, then their attributions should not differ. For further comments, see Sundararajan et al. [2017].

2.3 Relevant Modifications and Extensions

One issue with IG is the noisiness of the attribution image. This is attributed to sharp fluctuations in the gradient, sometimes called the shattered gradient problem [Balduzzi et al., 2017]. Smilkov et al. [2017] addresses this issue by randomly sampling near the image input and averaging the results, while Goh et al. [2021] incorporates the first order Taylor expansion to reduce nosiness. Another issue with integrated gradients is the choice of baseline. If the baseline is a black image, then for any black pixel, the $(x_i - x'_i)$ term will be zero, causing the attribution to be zero. One way to counteract this is to average two IG values, one with the black baseline, and another with a white baseline Tenserflow.com [2022]. Another approach is to use a distribution of baselines. Let X' be a probabilistic distribution defined on the input images, e.g. the uniform noise images. Define the *expected gradient* by:

$$\text{EG}_i(x, X', F) = \mathbb{E}_{x' \sim X'} \text{IG}_i(x, x', F)$$

Instead of a noise baseline, Erion et al. [2021] let X' be a uniform distribution over the training set, or some representative subset of it. The motivation is that the only images a model has been informed by are training images, so one could use those images as meaningful baselines of comparison. Individual training images are biased, but if the training set is

[3]Practically speaking, IG is relatively easy to implement. The IG is calculated by numerical integration with a recommended 20 to 300 calls of the gradient [Sundararajan et al., 2017].

balanced, EG would be unbiased due to the aggregate. If a second category of images were chosen for X', then EG could identify which inputs were responsible for a prediction of category, and not another. This metric has also been used as a regularization term on attributions during training [Erion et al., 2021] to promote properties of a model.

3 Remarks and Corrections on Original Paper

3.1 Remarks on Completeness, Path Definition

We first address a few claims of the original IG paper, [Sundararajan et al., 2017], to add mathematical clarifications. Sundararajan et al. [2017, Remark 2] states:

> *"Integrated gradients satisfies Sensivity(a) because Completeness implies Sensivity(a) and is thus a strengthening of the Sensitivity(a) axiom. This is because Sensitivity(a) refers to a case where the baseline and the input differ only in one variable, for which Completeness asserts that the difference in the two output values is equal to the attribution to this variable."*

To clarify, completeness implies sensitivity(a) for IG, and for monotone path methods in general. The form of IG guarantees that any input that does not differ from the baseline will have zero attribution, due to the $x_i - x_i'$ term in (2). If only one input differs from the baseline, and $F(x) \neq F(x')$, then the value $F(x) - F(x') \neq 0$ will be attributed to that input by completeness. However, completeness does not imply sensitivity(a) for general attribution methods, or for non-monotone path methods specifically.

In Sundararajan et al. [2017], monotone path methods (what they simply term path methods) are introduced as a generalization of the IG method. The section reads:

> *"Integrated gradients aggregate the gradients along the inputs that fall on the straightline between the baseline and the input. There are many other (non-straightline) paths that monotonically interpolate between the two points, and each such path will yield a different attribution method. For instance, consider the simple case when the input is two dimensional. Figure 1*[4] *has examples of three paths, each of which corresponds to a different attribution method.*
> *Formally, let $\gamma = (\gamma_1, ..., \gamma_n) : [0, 1] \to \mathbb{R}^n$ be a smooth function specifying a path in $\mathbb{R}^n$ from the baseline x' to the input x, i.e., $\gamma(0) = x'$, and $\gamma(1) = x$."*

By the referred figure, P_1 is identified as a path, but it is not smooth. It is simple enough to interpret smooth here to mean piecewise smooth. Note further that monotonicity is mentioned, and all examples in Figure 1 are monotone, but monotonicity is not explicitly included in the formal definition. The cited source on path methods, Friedman [2004], only considers monotone paths. Thus, we assume that Sundararajan et al. [2017] only considers monotone paths. The alternative is addressed in the discussion on Conjecture 1.

3.2 On the Uniqueness Claim

In the original IG paper, an important uniqueness claim is given as follows [Sundararajan et al., 2017, Proposition 2]:

> *"[Friedman, 2004] Path methods are the only attribution methods that always satisfy Implementation Invariance, Sensitivity(b), Linearity, and Completeness."*

The claim that every method that satisfies certain axioms must be a path method is an important claim for two reasons: 1) It categorically excludes every method that is not a path method from satisfying the axioms, and 2) It characterizes the form of methods satisfying the axioms. However, no proof of the statement is given, only the following remark (Remark 4):

> *"Integrated gradients correspond to a cost-sharing method called Aumann-Shapley [Aumann and Shapley, 1974]. Proposition 2 holds for our attribution problem because mathematically the cost-sharing problem corresponds to the attribution problem with the benchmark fixed at the zero vector."*

The cost sharing problem does correspond to the attribution problem with benchmark fixed at zero, *with some key differences*. To understand the differences, we will begin with some preliminaries, then review the original results in Friedman [2004] and give a rigorous statement of Sundararajan et al. [2017, Proposition 2]. We will then point out

[4] Sundararajan et al. [2017, Figure 1] is presented as Figure 4 in Appendix A

discrepancies between the function spaces that make the application of the results in Friedman [2004] neither automatic nor, in one case, appropriate.

Let $\Gamma(x, x')$ denote the set of all path functions projected onto their third component, so that x, x' are fixed and $\gamma \in \Gamma(x, x')$ is a function solely of t. We may write $\Gamma(x)$ when x' is fixed or apparent. Define the set of monotone path functions as $\Gamma^m(x, x') := \{\gamma \in \Gamma(x, x') | \gamma \text{ is monotone in each component}\}$. We can then define an *ensemble of path methods*:

Definition 5. For a fixed x', a BAM A is an ensemble of path methods if there exists a family of probability measures, indexed by $x \in [a, b]$, μ^x, each on $\Gamma(x)$, such that:

$$A(x, F) = \int_{\gamma \in \Gamma^m(x)} A^\gamma(x, F) d\mu^x(\gamma) \tag{3}$$

An ensemble of path methods is an attribution method where, for a given x, the attribution is equivalent to an average among a distribution of path methods. The distribution varies with x, but not with F.

In Friedman [2004], there are particular restrictions to the function space due to the game-theoretic context. In the game theoretic literature, attributions are called cost sharing methods, and arise in the context of a cost function F that gives the cost of satisfying the demands, x, of various agents. Each input x_i represents an agent's demand, $F(x)$ represents the cost of satisfying all demands, and the attribution to x_i represents that agent's share in the total cost. Due to the nature of the problem, $F(0) = 0$, naturally, and because increased demands cannot result in a lower total cost, $F(x)$ is non-decreasing in each component of x. Furthermore, only cost functions in C^1 are considered. To denote these restriction formally, we write that for a positive vector $b \in \mathbb{R}^n_+$, the set of attributed functions is denoted by $\mathcal{F}^0 = \{F \in \mathcal{F}(0, b) | F(0) = 0, F \in C^1, F \text{ non-decreasing in each component}\}$. The comparative baseline in this context is no demands, so $x' = 0$. Because an agent's demands can only increase the cost, an agent's demand should not have a negative attribution, thus only baseline attributions giving non-negative output are considered. We will denote the set of baseline attributions in Friedman [2004] by $\mathcal{A}^0 = \{A : [0, b] \times \mathcal{F}^0 \to \mathbb{R}^n_+\}$. The result is as follows:

Theorem 1. (Friedman [2004]'s Characterization Theorem)

The following are equivalent:

1. $A \in \mathcal{A}^0$ satisfies completeness, linearity[5], and sensitivity(b).
2. $A \in \mathcal{A}^0$ is an ensemble of monotone path methods.

Implementation invariance is not stated because all statements in the theorem are mathematical properties independent of implementation.

In contrast, IG's characterization claim applies to attribution on DL models, so many restrictions are removed. Define $\mathcal{F}^{\text{D}}$ to be the set of DL models where one output is considered, and define $\mathcal{A}^{\text{D}}$ to be the set of attribution methods defined on $\mathcal{F}^{\text{D}}$. Note that $F \in \mathcal{F}^{\text{D}}$ need not be non-decreasing, and its derivatives can have discontinuities (hence, not C^1). Additionally x' need not be 0, and $F(x')$ has no restrictions. Because $F \in \mathcal{F}^{\text{D}}$ is not monotone and $F(x)$ can decrease from the baseline, $A \in \mathcal{A}^{\text{D}}$ can take on negative values.

To give a rigorous statement of Proposition 2 in Sundararajan et al. [2017], we must interpret the claim: "path methods are the only attribution methods that always satisfy implementation invariance, sensitivity(b), linearity, and completeness." By "path methods", Sundararajan et al. [2017] cannot exclude ensembles of path methods, for then the statement is false by Theorem 1, which it references for proof. Neither can it mean non-monotone path methods, since Theorem 1 only addresses monotone path methods, and it is supposed to apply immediately. Thus we will interpret "path methods" as in Theorem 1, as an ensemble of monotone path methods. We now state the characterization theorem found in Sundararajan et al. [2017]:

Claim 1. (Sundararajan et al. [2017]'s Characterization Claim) Fix $x' \in [a, b]$. Suppose $A \in \mathcal{A}^{\text{D}}$ satisfies completeness, linearity, sensitivity(b), and implementation invariance. Then A is an ensemble of monotone path methods.

This claim is false. Note that monotone and non-monotone path methods satisfy completeness[6], linearity, sensitivity(b), and implementation invariance. Fixing the baseline to zero and $[a, b] = [0, 1]^n$, there exist a non-monotone path $\omega(t)$ and non-decreasing F s.t. $A^\omega(x, x', F)$ has negative components. However, if path $\gamma(t) = \gamma(x, x', t)$ is monotone and F is non-decreasing, $\frac{\partial \gamma_i}{\partial t} \geq 0$ and $\frac{\partial F}{\partial x_i} \geq 0$, $\forall i$. By Eq. 1, $A^\gamma(x, x', F) \geq 0$ for monotone γ and non-decreasing F,

[5] Friedman [2004] uses a weaker form of linearity: $A(x, F + G) = A(x, F) + A(x, G)$.

and any ensemble of monotone path methods would be non-negative. Thus, A^ω is not an ensemble of monotone path methods. For a full proof, see Appendix B.

Why did this happen? Note that in the context of Theorem 1, this counterexample is disallowed. $\mathcal{A}^0$ only includes attributions that give non-negative values since cost shares do not decrease as x moves away from the baseline. Non-monotone path attributions can give negative values, even when F is non-decreasing and $x' = 0$, so they are prohibited from the beginning. In the DL context, however, functions are not monotone, and the function could increase or decrease from the baseline. This wider class of functions necessitated allowing attributions to be negative. Because no additional constraints were imposed, non-monotone path methods were allowed.

The above example shows that the set of BAMs satisfying axioms 3-5 cannot be characterized as an ensemble of path methods over Γ^m. Since the counter example was a non-monotone path method, perhaps the set BAMs can be characterized as an ensemble of path methods over Γ.

Conjecture 1. Fix x'. The following are equivalent:

- $A \in \mathcal{A}^{\mathrm{D}}$ satisfies completeness, linearity, sensitivity(b), and implementation invariance.
- $A \in \mathcal{A}^{\mathrm{D}}$ is an ensemble of path methods, where the maximal path length of the support of μ^x is bounded.[7]

If Conjecture 1 were true, it would somewhat preserve the thrust of Claim 1: that BAMs satisfying axioms 3-5 are path methods. However, it is not clear how Theorem 1 can be used to support Conjecture 1, since it proves characterizations exclusively with monotone path ensembles. On the other hand, it is an open question whether conjecture one is false, that is, there is a BAM satisfying axioms 3-5 that is not an ensemble of path methods.

Even if we do not have any path characterization for BAMs satisfying axioms 3-5, we submit some insights into BAMs satisfying axioms 4 and 5.

Lemma 1. Suppose a BAM A satisfies linearity and sensitivity(b). Then $A(x, x', F)$ is a function solely of x, x', and the gradient of F. Furthermore, $A_i(x, x', F)$ is a function solely of x, x' and $\frac{\partial F}{\partial x_i}$.

3.3 Non-Decreasing Positivity

Another way to extend Theorem 1 is to provide further constraints on $\mathcal{A}^{\mathrm{D}}$. To this end, we introduce the axioms of *non-decreasing positivity* (NDP). We say that F is non-decreasing from x' to x if $F(\gamma(t))$ is non-decreasing for every monotone path $\gamma(t) \in \Gamma(x, x')$ from x' to x. We can then define NDP as follows:

Definition 6. A BAM A satisfies NDP if $A(x, x', F) \geq 0$ whenever F is non-decreasing from x' to x.

F being non-decreasing from x' to x is analogous to a cost function being non-decreasing in the cost sharing context. NDP is then analogous to requiring the cost share function to be non-negative. Put another way, NDP states that if $F(y)$ does not decrease when any input y_i moves closer to x_i from x'_i, then $A(x, x', F)$ should not give negative values to any input. The addition of NDP enables Theorem 1 to extend closer to the DL context.

Theorem 2. (Characterization Theorem with NDP) Let x' be fixed. Define $\mathcal{F}^1$ to be the intersection of functions in $\mathcal{F}^D$ and C^1. Define $\mathcal{A}^1$ to be the set of baseline attributions with the domain restricted to $\mathcal{F}^1$. Then the following are equivalent:

1. $A \in \mathcal{A}^1$ satisfies completeness, linearity, sensitivity(b), and NDP.
2. $A \in \mathcal{A}^1$ is an ensemble of monotone path methods.

A sketch of the proof is as follows. Let x be fixed, and $F \in \mathcal{F}^1$. It can be shown that the behavior of F outside of $[x, x']$ is irrelevant to $A(x, x', F)$. Using this, apply a coordinate transform T that maps $[x, x']$ onto $[0, |x - x'|]$, so that $A(x, x', F) = A^0(0, |x - x'|, F^0)$, where A^0, F^0 have proper domains to apply Theorem 1. F^0 is C^1 and defined on a compact domain, so it's derivative is bounded, and there exists $c \in \mathbb{R}^n$ such that $F^0(y) + c^T y$ is non-decreasing in y. Apply Theorem 1 to $A^0(x, x', F^0(y) - c^T y)$ and simplify to get a characterization for $A(x, x', F)$ in terms of $\Gamma[0, |x - x'|]$ and F^0. Reverse the transform to get the characterization in terms of $\Gamma(x, x')$ and F.

To expand Theorem 2 further to non-C^1 functions, we will consider a limited subset of DL models with non-continuous derivatives. consider the set of neural networks with piecewise linear activation functions such as ReLU and OutMax. It

[6]Path methods satisfy completeness because $\sum_i A_i^\gamma(x, x', F) = \int_0^1 \nabla F * d\gamma = F(x) - F(x')$ by the fundamental theorem for line integrals.

[7]For the necessity of bounding maximal path length, see the Appendix D

was shown by Chu et al. [2018] that such functions are a composition of a finite number of locally linear classifiers with convex polytope boundaries. We will consider the same set, defining $\mathcal{F}^2$ to be any continuous DL model F where F's domain can be partitioned into a number of convex polytopes, and F linear in each polytope. We then define $\mathcal{A}^2$ to be any $A \in \mathcal{A}^{\text{D}}$ with domain limited to $F \in \mathcal{F}^2$.

Theorem 3. (Extension to Simple non-C^1 Functions)

Let x' be fixed. Suppose $A \in \mathcal{A}^2$ satisfies completeness, linearity, sensitivity(b), and NDP. Suppose further that $F \in \mathcal{F}^2$, and that for some x, ∇F is defined for almost every γ (according to μ^x). Then $A(x, F)$ is equivalent to the usual ensemble of path methods.

3.4 Lipschitz Continuity

DL models can be extremely sensitive to slight changes in the input image Goodfellow et al. [2014], [Chaubey et al., 2020]. It stands to reason that IG should also be sensitive in x for sensitive models, and less sensitive in the input for less sensitive models. We study the sensitivity of IG for two extremes, one example where the gradient is discontinuous, and another where the gradient is well behaved:

Theorem 4. Let x' be fixed. If F has the usual discontinuities due to ReLu or Max functions, then $IG(x, F)$ may fail to be Lipschitz continuous in x. If ∇F is Lipschitz continuous, then IG(x, F) is Lipschitz continuous in x.

4 Distribution Baseline Axioms

The axioms introduced in IG do not necessarily apply to a distributional baseline version of IG, due to the lack of a single baseline. Some, like sensitivity(b) and linearity, have obvious analogues. Sensitivity(a), completeness, and symmetry preserving, however, do not. Below we identify probabilistic analogues of the sensitivity(a), completeness, and symmetry preserving axioms, all of which are satisfied by Expected Gradients. Some necessary preliminaries: let $\mathcal{D}$ be the set of distributions on $[a, b]$. Let $\mathcal{E}$ be the set of distributional attributions, so that for $E \in \mathcal{E}$, $E : [0, b] \times \mathcal{D} \times \mathcal{F} \to \mathbb{R}^n$. Let $E \in \mathcal{E}$, $X' \sim D$, and $F, G \in \mathcal{F}$:

1. Sensitivity(a): Suppose X varies in exactly one input, X_i, so that $X_j = x_j$ for all $j \neq i$, and $\mathbb{E}F(X') \neq F(x)$. Then $E_i(x, X', F) \neq 0$.
2. Completeness: For all F, x, X', we have: $\sum_{i=1}^{n} E_i(x, X', F) = F(x) - \mathbb{E}F(X')$.
3. Symmetry Preserving: For a given i, j, define x^* by swapping the values of x_i and x_j. Now suppose that for all x, $F(x) = F(x^*)$. Then whenever X'_i and X'_j are symmetric with respect to D, $x_i = x_j$, we have $E_i(x, X', F) = E_j(x, X', F)$.

5 Internal Neuron Attributions

5.1 Applying IG to internal neurons

Previous work by Lundstrom et al. [2022] applies IG to internal neuron layers to obtain internal neuron attributions. We review their results before discussing extensions. Suppose F is a single output of a feed forward neural network, with $F : [a, b] \to \mathbb{R}$. We can separate F at an internal layer such that $F(x) = G(H(x))$. Here $H : [a, b] \to \mathbb{R}^m$ is the first half of the network outputting the value of an internal layer of neurons, and $G : \mathbb{R}^m \to \mathbb{R}$ is the second half of the network that would take the internal neuron values as an input. If we perform IG on G, we can obtain attributions for an internal layer of neurons. If the network uses the ReLU activation function, then a natural baseline would be 0, representing no features present. Taking $H(x)$ as the input to G, we can write the IG attribution of H_i as:

$$\text{IG}_i(H(x), G) = H_i(x) \int_0^1 \frac{\partial G}{\partial H_i}(tH(x))dt \tag{4}$$

Note that this method does not take into account the first half of the network, H, except its outputs at the data point x. Below we consider a path method that is informed by H.

5.2 Decomposition Method

Consider our previous setup of $F(x) = G(H(x))$, $\gamma(\alpha) = x' + \alpha(x - x')$. Now note $\frac{\partial F}{\partial x_i} = \sum_j \frac{\partial G}{\partial H_j} \frac{\partial H_j}{\partial x_i}$, and observe:

$$\begin{aligned} F(x) - F(x') &= \sum_i IG_i(x, F) \\ &= \sum_i (x_i - x_i') \int_0^1 \frac{\partial F}{\partial x_i}(\gamma) dt \\ &= \sum_i (x_i - x_i') \int_0^1 \sum_j \frac{\partial G}{\partial H_j}(H(\gamma)) \frac{\partial H_j}{\partial x_i}(\gamma) dt \\ &= \sum_{i,j} (x_i - x_i') \int_0^1 \frac{\partial G}{\partial H_j}(H(\gamma)) \frac{\partial H_j}{\partial x_i}(\gamma) dt \\ &=: \sum_{i,j} {}_j\text{IG}_i(x, F) \end{aligned} \tag{5}$$

Explaining the notation used at the end, we define ${}_j\text{IG}_i(x, F) = (x_i - x_i') \int_0^1 \frac{\partial G}{\partial H_j}(H(\gamma)) \frac{\partial H_j}{\partial x_i}(\gamma) dt$, and we can think of this as the portion of the IG attribution to input x_i that flowed through neuron j. If we fix j, then ${}_j\text{IG}_i(x, F)$ is a function of i, or the input pixels, and represents the portion of the attribution map $\text{IG}(x, F)$ that is associated with neuron j. Summing up the attribution sub-maps for each neuron yields the original attribution map, $\text{IG}(x, F)$.

Finally, let us define an augmented path, $\gamma'(\alpha) = H(\gamma(\alpha)))$. $\gamma'(\alpha)$ is the path that results from pushing the path γ in the input space through H to obtain a new path in the internal neuron space. With this observation, we define a new path method for the the neurons based on the path γ'. We denote this $A^{\gamma'}(H(x), G)$, and show:

$$\begin{aligned} &\sum_i {}_jIG_i(x, F) \\ &= \int_0^1 \frac{\partial G}{\partial H_j}(H(\gamma) \times \sum_i \left[\frac{\partial H_j}{\partial x_i}(\gamma)(x_i - x_i') \right] dt \\ &= \int_0^1 \frac{\partial G}{\partial \gamma_j'}(\gamma') \frac{\partial \gamma_j'}{\partial t} dt = A_j^{\gamma'}(H(x), G_j) \end{aligned} \tag{6}$$

The above indicates that summing up an attribution sub-map for a particular neuron yields a path method attribution for that neuron attribution. This new formulation of neuron attributions is similar to the previous one, although with an augmented path determined by H. This augmented path allows the first half of the network, H, to inform the neuron attributions. The fact that incorporating H in this way yields a non-monotone path method suggests that non-monotone path methods may have some utility.

Setting ${}_j\text{IG}(x, F) := A_j^{\gamma'}(x, G)$, there is a fundamental relationship that holds between the defined methods above:

$$\begin{aligned} F(x) - F(x') &= \sum_{i,j} {}_j\text{IG}_i(x, F) \\ &= \sum_i \text{IG}_i(x, F) = \sum_j {}_j\text{IG}(x, F) \end{aligned} \tag{7}$$

This result can extend beyond one intermediate layer, up to and including every individual layer on a feed forward neural network. One can also decompose the IG map with regards to neuron partitions in a particular layer, or to a set of neural pathways involving multiple intermediate layers.

% pruned	Accuracy after pruning		
	Randomly	By IG ↑	By IG ↓
0	88.59	88.59	88.59
10	86.18	85.91	82.94
30	80.48	82.55	73.15
50	62.29	71.59	50.98
70	49.83	58.80	36.57
90	20.66	25.63	21.48
99	10.86	13.38	08.29
100	10.00	10.00	10.00

Table 1: Pruning neurons by IG values versus random pruning. IG ↑ means pruning neurons by IG values in ascending order. IG ↓ means pruning neurons by IG values in descending order.

6 Experimental Results

In this section, we conduct experiments on the Fashion MNIST dataset [Xiao et al., 2017], which consists of 28×28 arrays of grayscale pixel images classified into 10 categories of clothing. We apply IG to the training images with both black and random baselines. See Appendix H for example images. All experiments are conducted with a simple model which consists of two convolutional layers and two feed forward layers described in Appendix J.

6.1 Computation of IG on Internal Neurons

In these experiments, we calculate internal neurons attributions and IG sub-maps for a layer of internal neurons. We use the decomposition method proposed in Section 5.2, and we attribute with respect to the output of the first feed forward layer, which has a total of 64 neurons. To compute the maps, we compute ${}_j\text{IG}_i(x, F)$ for each pixel i and internal neuron $j \in \{1 \dots 64\}$. We find these maps for the output of F corresponding to the correct ground-truth category. To compute the neuron attributions we take $\sum_{ij} \text{IG}_i(x, F) =_j \text{IG}(x, F)$. The internal neuron attributions reveal the contribution of each neuron towards the final classification confidence, F. Positive attributions show that the corresponding neurons are responsible for increasing the confidence of the correct class. One natural application of this is neuron pruning. Intuitively, neurons with small attribute values do not contribute to the classification confidence. To verify this hypothesis, we zero out neurons based on the ranking of their values of IG attributes and compare this approach with random pruning of neurons.

The experiment has two parts: we first prune the neurons from the smallest IG value to the largest IG value and compare with random pruning. We then prune the neurons with the reversed ranking and compare with random pruning again. Table 1 demonstrates the results of pruning by IG value versus random pruning. The first column shows the proportion of neurons being zeroed out. We prune the neurons by their IG values in ascending order, i.e., the least important neurons first. It can be seen that compared with random pruning (check column 2 and column 3), the pruned by IG values model performs better since we first trim off the neurons that contribute least to the classification task. On the contrary, if we prune the neurons by IG values in a descending order, i.e., prune the most contributing ones first, pruning by IG values hurts the performance more than random pruning with the same number of neurons being zeroed out (check column 2 and column 4).

6.2 Per Class IG on Internal Neurons

We can also find the IG attributes on internal neurons for a specific class. In other words, we are interested in the neurons which are more responsible for the specific class than others. This can be done by considering one output and computing the aggregated IG attributes only with respect to examples of the certain class. In this experiment, we focus on class 7 which is Sneaker.

Figure 1 depicts the results of the experiment. Using a similar method to the previous section, in this section we: prune from low to high (keep the performance)(Left); and prune for high to low (kill the performance)(Right). In each sub-figure, we show the median testing accuracy and Sneaker testing accuracy for the model after random pruning and by IG respectively. On the left panel, it can been seen that by removing the neurons which are not responsible for Sneakers, we can keep the performance of Sneakers all the way until few neurons are left. It can be also seen that random pruning hurts the performance for all classes at the same time. In the reverse, we can also harm the performance of Sneakers only while keeping the performance of other classes by pruning the neurons starting with the largest IG. Right panel shows that we can destroy the testing accuracy of Sneakers only with one third of the neurons being pruned.

6.3 IG on Internal Neurons for a Specific Region

Recall (7) shows the IG decomposition identity. We can further compute IG values for internal neurons with respect to a specific region $\mathcal{B}$, i.e., $\sum_{i\in\mathcal{B}} {}_j IG_i(x, F)$ where j is the index of the internal neuron. This decomposition is particularly useful for understanding the attribution of the internal neuron with respect to a specific feature. For example, the shoulder of a T-shirt, or the round arch of a shoe. In this experiment, we first compute the original IG attribution over the input image for a certain class: Sneaker. We then arbitrarily draw a bounding box and find the IG attributes of the internal neurons with respect to the pixels inside the bounding box only. Figure 2 (Left) shows the IG attributes over the input image and the yellow bounding box.

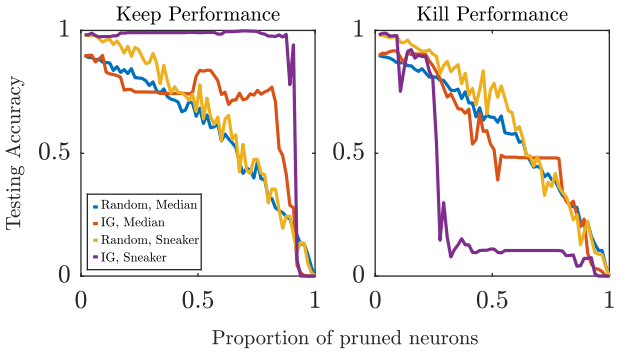

Figure 1: Testing accuracy when neurons are pruned according to their IG values corresponding to the class *Sneaker*. "Random, Median", "IG, Median" report median accuracies of all classes and the neurons are pruned randomly and by their IG value respectively. "Random, Sneaker", "IG, Sneaker" report accuracy of class Sneaker only and the neurons are pruned randomly and by their IG value respectively. Left: Prune neurons by their IG values in ascending order. Right: Prune neurons by their IG values in descending order.

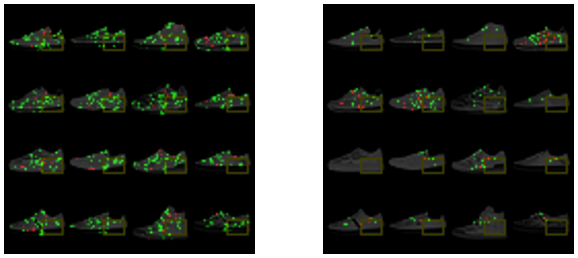

Figure 2: Left: IG attributes with respect to the sneaker images. Green dots show positive IG attributes and red dots show negative IG attributes. Bounding boxes are shown in yellow. Right: Recomputed IG attributes with respect to the sneaker images after internal neurons being pruned.

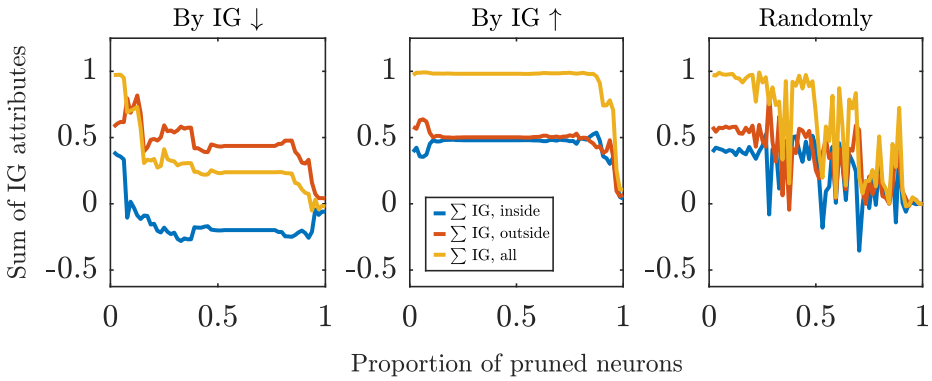

Figure 3: Summation of the recomputed IG attributes inside the bounding box, outside the bounding box and both. Summations are averaged over 64 samples chosen from testing set. Left: Pruning by the IG ranking in descending order. Middle: Pruning by the IG ranking in ascending order. Right: Randomly pruning.

We seek to test for a correlation between the regional IG neuron values, and the IG map behavior on the region. To do this, we use a similar technique: we again zero out the internal neurons based on rank for the region and recompute the IG values over the image. Supposedly, if the most contributing neurons are zeroed out, we should see almost no positive recomputed IG value in the bounding box. Figure 2 (Right) confirms our conjecture as there are almost no positive IG value in the bounding box. To better illustrate this example, we compute the summation of recomputed IG values both inside and outside the bounding box. We use black images as baseline and therefore the recomputed IG attributes should sum up to one. Similar to previous sections, we zero out the internal neurons by IG rankings (both high to low and low to high) and randomly. Figure 3 (Left) suggests that as more neurons are pruned, the summation of recomputed IG attributes inside the bounding box drops to and below zero rapidly. This shows our pruning is extremely effective and after the first few most-contributing neurons to the bounding box are zeroed out, there are no (positive) IG attributes in the bounding box anymore. Figure 3 (Middle) suggests that as we prune more neurons, the summation of IG attributes inside and outside the bounding box stay almost the same. This is not unexpected since we start pruning from the least contributing neurons. Figure 3 (Right) shows random pruning is not selective. In other words, both the recomputed IG values inside and outside the bounding box decrease almost at the same pace.

7 Link to Code

The code for the experiments can be found at:
`https://github.com/optimization-for-data-driven-science/XAI/`

References

Gao Huang, Zhuang Liu, Laurens Van Der Maaten, and Kilian Q Weinberger. Densely connected convolutional networks. In *Proceedings of the IEEE conference on computer vision and pattern recognition*, pages 4700–4708, 2017.

Shaoqing Ren, Kaiming He, Ross Girshick, and Jian Sun. Faster r-cnn: towards real-time object detection with region proposal networks. *IEEE transactions on pattern analysis and machine intelligence*, 39(6):1137–1149, 2016.

Alexey Bochkovskiy, Chien-Yao Wang, and Hong-Yuan Mark Liao. Yolov4: Optimal speed and accuracy of object detection. *arXiv preprint arXiv:2004.10934*, 2020.

David Baehrens, Timon Schroeter, Stefan Harmeling, Motoaki Kawanabe, Katja Hansen, and Klaus-Robert Müller. How to explain individual classification decisions. *The Journal of Machine Learning Research*, 11:1803–1831, 2010.

Matthew D Zeiler and Rob Fergus. Visualizing and understanding convolutional networks. In *European conference on computer vision*, pages 818–833. Springer, 2014.

Jost Tobias Springenberg, Alexey Dosovitskiy, Thomas Brox, and Martin Riedmiller. Striving for simplicity: The all convolutional net. *arXiv preprint arXiv:1412.6806*, 2014.

Avanti Shrikumar, Peyton Greenside, and Anshul Kundaje. Learning important features through propagating activation differences. In *International Conference on Machine Learning*, pages 3145–3153. PMLR, 2017.

Alexander Binder, Grégoire Montavon, Sebastian Lapuschkin, Klaus-Robert Müller, and Wojciech Samek. Layer-wise relevance propagation for neural networks with local renormalization layers. In *International Conference on Artificial Neural Networks*, pages 63–71. Springer, 2016.

Bolei Zhou, Aditya Khosla, Agata Lapedriza, Aude Oliva, and Antonio Torralba. Learning deep features for discriminative localization. In *Proceedings of the IEEE conference on computer vision and pattern recognition*, pages 2921–2929, 2016.

Luisa M Zintgraf, Taco S Cohen, and Max Welling. A new method to visualize deep neural networks. *arXiv preprint arXiv:1603.02518*, 2016.

Mukund Sundararajan, Ankur Taly, and Qiqi Yan. Axiomatic attribution for deep networks. In *International Conference on Machine Learning*, pages 3319–3328. PMLR, 2017.

Gabriel Erion, Joseph D Janizek, Pascal Sturmfels, Scott M Lundberg, and Su-In Lee. Improving performance of deep learning models with axiomatic attribution priors and expected gradients. *Nature Machine Intelligence*, pages 1–12, 2021.

Eric J Friedman. Paths and consistency in additive cost sharing. *International Journal of Game Theory*, 32(4):501–518, 2004.

Robert J. Aumann and Lloyd S. Shapley. *Values of Non-Atomic Games*. Princeton University Press, Princeton, NJ, 1974.

David Balduzzi, Marcus Frean, Lennox Leary, JP Lewis, Kurt Wan-Duo Ma, and Brian McWilliams. The shattered gradients problem: If resnets are the answer, then what is the question? In *International Conference on Machine Learning*, pages 342–350. PMLR, 2017.

Daniel Smilkov, Nikhil Thorat, Been Kim, Fernanda Viégas, and Martin Wattenberg. Smoothgrad: removing noise by adding noise. *arXiv preprint arXiv:1706.03825*, 2017.

Gary SW Goh, Sebastian Lapuschkin, Leander Weber, Wojciech Samek, and Alexander Binder. Understanding integrated gradients with smoothtaylor for deep neural network attribution. In *2020 25th International Conference on Pattern Recognition (ICPR)*, pages 4949–4956. IEEE, 2021.

Tenserflow.com. Integrated gradients, 2022. URL `https://www.tensorflow.org/tutorials/interpretability/integrated_gradients`.

Lingyang Chu, Xia Hu, Juhua Hu, Lanjun Wang, and Jian Pei. Exact and consistent interpretation for piecewise linear neural networks: A closed form solution. In *Proceedings of the 24th ACM SIGKDD International Conference on Knowledge Discovery & Data Mining*, pages 1244–1253, 2018.

Ian J Goodfellow, Jonathon Shlens, and Christian Szegedy. Explaining and harnessing adversarial examples. *arXiv preprint arXiv:1412.6572*, 2014.

Ashutosh Chaubey, Nikhil Agrawal, Kavya Barnwal, Keerat K Guliani, and Pramod Mehta. Universal adversarial perturbations: A survey. *arXiv preprint arXiv:2005.08087*, 2020.

Daniel Lundstrom, Alexander Huyen, Arya Mevada, Kyongsik Yun, and Thomas Lu. Explainability tools enabling deep learning in future in-situ real-time planetary explorations. *arXiv preprint arXiv:2201.05775*, 2022.

Han Xiao, Kashif Rasul, and Roland Vollgraf. Fashion-mnist: a novel image dataset for benchmarking machine learning algorithms, 2017.

Appendix

A Figure 1 from Sundararajan et al. [2017]

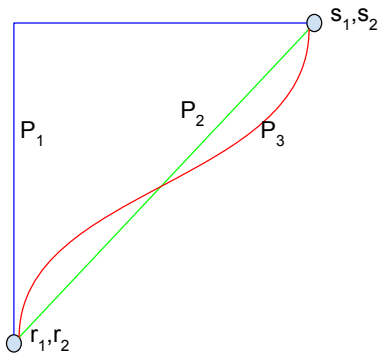

Figure 4: Three paths between an a baseline (r_1, r_2) and an input (s_1, s_2). Each path corresponds to a different attribution method. The path P_2 corresponds to the path used by integrated gradients.

B Counterexample to Claim 1

Let $F(x_1, x_2) = x_1 x_2$ be defined on $[0, 1]^2$, $x' = (0, 0)$, $x = (1, 0)$. Suppose that A^γ is defined by a monotone path. Note that $\frac{\partial F}{\partial x_i} \geq 0$, $\frac{\partial \gamma_i}{\partial t} \geq 0$ for all i. Thus $A^\gamma(x, x', F) \geq 0$ by Eq. 5. Thus any ensemble of monotone path methods has a non-negative output for the input (x, x', F).

Let γ' be the path that travels via a straight line from $(0, 0)$ to $(0, 1)$, then to $(1, 1)$, and ends at $(1, 0)$. $A^{\gamma'}$ satisfies completeness, linearity, sensitivity(b), and implementation invariance. $A^{\gamma'}(x, x', F) = (1, -1) \ngeq 0$. Thus not every baseline attribution that satisfies completeness, linearity, sensitivity(b), and implementation invariance is a probabilistic ensemble of monotone path methods.

C Proof of Lemma 1

Proof. Suppose A satisfies linearity and sensitivity(b). Let $F, G \in \mathcal{F}$ be such that $\frac{\partial F}{\partial x_i} = \frac{\partial G}{\partial x_i}$ for some i, and let and $x, x' \in [0, b]$. Then $\frac{\partial (F-G)}{\partial x_i} = 0$, and by sensitivity(b), $A_i(x, x', F) - A_i(x, x', G) = A_i(x, x', F - G) = 0$. Thus $A_i(x, x', F) = A_i(x, x', G)$, and A_i is a function solely of x, x' and $\frac{\partial F}{\partial x_i}$. By extension, $A(x, x', F)$ is a function solely of x,x', and ∇F.

□

D Comment on Conjecture 1

If no qualifications are put on the set of paths that μ^x is supported on, then A may be undefined, or take on infinite values and contradict completeness. Consider the following example. Let $n = 2$, $[a, b] = [(0, 0), (1, 1)]$. Let $F(y) = y_1 y_2$, $x = (1, 1)$, $x' = (0, 0)$. Define the path $\gamma^n(x, x', t)$ to be the path obtained by traveling completely around the boundary of the domain clockwise n times, then following the straight line from $(0, 0)$ to $(1, 1)$. We define $\gamma^{-n}(x, x', t)$ similarly to γ^n, but with counterclockwise paths. $A^{\gamma^0}(x, x', F) = (0.5, 0.5)$. $A^{\gamma^n}(x, x', F) = (0.5 + n, 0.5 - n)$, $n \in \mathbb{Z}$. Now define the support of $\mu^x(\gamma)$ to be $\{\gamma^{(-2)^k} : k \in \mathbb{Z}\}$. We then define μ^x on it's support to be $\mu^x(\gamma^{(-2)^k}) = \frac{1}{2^k}$.

$$
\begin{aligned}
&A(x, x', F) \\
&= \int_{\gamma \in \Gamma(x,x')} \mathcal{A}^{\gamma}(x, x', F) d\mu^{x}(\gamma) \\
&= \sum_{k=1}^{\infty} (0.5 + (-2)^k, 0.5 - (-2)^k) \frac{1}{2^k} \\
&= \sum_{k=1}^{\infty} (\frac{0.5}{2^k} + (-1)^k, \frac{0.5}{2^k} - (-1)^k)
\end{aligned}
$$

The above sum is not convergent in either component, so $A, x, x', F)$ is not defined.

A similar construction may yield $A(x, x', F) = (\infty, -\infty)$, contradicting completeness.

E Proof of Theorem 2

Proof. We begin by supposing the assumptions. Let x' be fixed, $\mathcal{F}^1$ and $\mathcal{A}^1$ be as stipulated, and $A \in \mathcal{A}^1$. We introduce the notation $\mathcal{A}^1(c, d)$, $c, d \in \mathbb{R}^n$, to be defined as the set $\mathcal{A}^1$, but with specified region $[c, d]$ instead of $[a, b]$. The set $\mathcal{F}^1(c, d)$ is defined likewise.

$2) \rightarrow 1)$: Suppose A is an ensemble of monotone path methods as in the theorem statement. It is trivial to show that A satisfies linearity, completeness, and sensitivity(b). Suppose F is non-decreasing from x' to some x. Then for any monotone path γ from x' to x, $A^{\gamma}(x, x', F) \geq 0$. Thus $A(x, x', F) \geq 0$, and A satisfies NDP.

$1) \rightarrow 2)$: Let A satisfy completeness, linearity, sensitivity(b), and NDP. Let $F \in \mathcal{F}^1(a, b)$ and $x \in [a, b]$. WLOG, we may assume that $F(x') = 0$, since if not, consider $G(y) := F(y) - x'$ and apply Lemma 1.

Our strategy will be to first define a transform such that A can be represented as a baseline attribution with baseline 0. Define $T : \mathbb{R}^n \rightarrow \mathbb{R}^n$ as $T_i(y) = (y_i - x'_i) * (-1)^{\mathbb{1}_{x'_i > x_i}}$. One can think of T as a transform from the baseline x' space to the baseline 0 space. T transforms $[a, b]$, by shifting and reflections about axes, into some other rectangular prism $[c, d]$, for some $c, d \in \mathbb{R}^n$. More importantly, T transforms x' to 0 and x to $|x - x'|$. Specifically, we get $T([x, x']) = [0, |x - x'|]$, with $T(x') = 0$ and $T(x) = |x - x'|$. Note further that T transforms the set of monotone paths from x' to x into the set of monotone paths from 0 to $|x - x'|$, or $T(\Gamma^m(x, x')) = \Gamma^m(0, |x - x'|)$. T is one-to-one and has a well defined inverse over $\mathbb{R}^n$. So one can think of T^{-1} as a transform from the baseline 0 space to the baseline x' space.

For $y, y' \in [c, d]$, $G \in \mathcal{F}^1(c, d)$, define $A' \in \mathcal{A}^1(c, d)$ by $A'(y, y', G) := A(T^{-1}(y), T^{-1}(y'), G * T)$. Essentially A' is a reformulation of A in the baseline 0 space. By definition, $A(x, x', F) = A'(|x - x'|, 0, F * T^{-1})$. A' satisfies completeness, linearity, sensitivity(b), and NDP.

Note that to apply Theorem 1, we must restrict the domain of A' to not include inputs with negative components. If we restrict the domain of A', it is not clear that this attribution will behave the same. It seems possible that the attribution $A'(x, x', F)$ depends on the behavior of F in the domain we want to remove. If this were the case, issues could arise, such as the restricted A' not being equivalent to the unrestricted A'. To address this issue, we turn to the development of an important lemma.

Lemma 2. If $A \in \mathcal{A}^1$ satisfies completeness, linearity, sensitivity(b), and NDP, then $A(x, x', F)$ is determined by x, x' and the behavior of F inside [x,x'].

Proof. Suppose $G, H \in \mathcal{F}^1$ have the same behavior in $[a, b]$. So for $y \in \mathbb{R}$, $G(y) - H(y) = 0 = H(y) - G(y)$. Thus both are non-decreasing from x' to x. Because A satisfies NDP, $A(x, x', H - G) \geq 0$, and $A(x, x', G - H) = -A(x, x', H - G) \geq 0$. Thus $0 = A(x, x', G) - A(x, x', H)$, and $A(x, x', G) = A(x, x', H)$. □

Now we define a BAM to apply Theorem 1 on. Define $A^0 : [0, T(x)] \times \mathcal{F}^0(0, T(x))$ as such: for $y \in [0, T(x)]$, $F^0 \in F^0(0, T(x))$, we let $H \in \mathcal{A}^1$ be any function such that $H \equiv F$ when restricted to $[0, T(x)]$, and set $A^0(y, F) := A'(y, 0, H)$. A^0 is a properly defined BAM by Lemma 2. Note that for $F \in A^1$ with $F(0) = 0$, F non decreasing, and $y \in [0, T(x)]$, we may go backwards and say $A'(x, 0, F) = A^0(x, F)$. Furthermore, $A^0 \in \mathcal{A}^0$ satisfies completeness, linearity, sensitivity(b).

Write $F^0 = F * T^{-1}$. F^0 is a C^1 function defined on a compact domain, so ∇F^0 is bounded. So there exists $c \in \mathbb{R}^n$ such that $\nabla(F^0(y) + c^T y) = \nabla F^0 + c \geq 0$ on the compact domain. This implies that $F^0(y) + c^T y$ is non-decreasing, C^1, with $F^0(0) = 0$. So $F^0(y) + c^T y \in \mathcal{A}^0$. Employing Theorem 1, there exists a μ such that:

$$\begin{aligned}
&A_i(x, x', F(y) + c^T T(y)) \\
=&A_i'(T(x), 0, F^0(y) + c^T y) \\
=&A_i^0(T(x), F^0(y) + c^T y) \\
=&\int_{\gamma \in \Gamma^m(T(x),0)} A_i^\gamma(T(x), 0, F^0(y) + c^T y) \times d\mu(\gamma)
\end{aligned}$$

Inspecting the interior term, we find that for γ a monotone path from 0 to $T(x)$,

$$\begin{aligned}
&A_i^\gamma(T(x), 0, F^0(y) + c^T y) \\
=&\int_0^1 [\frac{\partial F^0}{\partial \gamma_i} + c_i] \frac{\partial \gamma_i}{\partial t} dt \\
=&\int_0^1 \frac{\partial F * T^{-1}}{\partial \gamma_i} \times \frac{\partial \gamma_i}{\partial t} dt + c_i(T_i(x) - 0) \\
=&\int_0^1 \frac{\partial F}{\partial (T^{-1} * \gamma)_i}(T^{-1}(\gamma(t)) \times \frac{\partial T_i^{-1}}{\partial \gamma_i}(\gamma(t)) \times \frac{\partial \gamma_i}{\partial t} dt + c_i(T_i(x) - 0) \\
=&\int_0^1 \frac{\partial F}{\partial (T^{-1} * \gamma)_i}(T^{-1}(\gamma(t))) \times \frac{\partial (T^{-1} * \gamma)_i}{\partial t} dt + c_i T_i(x) \\
=&A_i^{(T^{-1} * \gamma)}(x, x', F) + c_i T_i(x)
\end{aligned}$$

Recalling that $\Gamma^m(T(x), 0) = T(\Gamma^m(x, x'))$, and combining previous results, we have,

$$\begin{aligned}
&A_i(x, x', F(y)) + A_i(x, x', c^T T(y)) \\
=&A_i(x, x', F(y) + c^T T(y)) \\
=&\int_{\gamma \in \Gamma^m(T(x),0)} A_i^{(T^{-1} * \gamma)}(x, x', F) + c_i T_i(x) d\mu(\gamma) \\
=&\int_{\gamma \in \Gamma^m(x,x')} A_i^\gamma(x, x', F) + c_i T_i d\mu(\gamma) \\
=&\int_{\gamma \in \Gamma^m(x,x')} A_i^\gamma(x, x', F) d\mu(\gamma) + c_i T_i(x)
\end{aligned}$$

From a previous result, $A_i(x, x', G)$ is a function only of x, x' and $\frac{\partial G}{\partial x_i}$. So $A_i(x, x', c^T T(y)) = A_i(x, x', c_i T_i(y))$. By sensitivity(b), $A_j(x, x', c_i T_i(y)) = 0$ for $j \neq i$. So by completeness, $A_i(x, x', c_i T_i(y)) = c_i T_i(x) - c_i T_i(x') = c_i T_i(x)$. Subtracting the term from both sides of the above equation above yields the result.

Note that A'' is determined by the choice of x and x', since T is determined by x, x'. So for any $F \in \mathcal{F}^1$, we get the same μ defined on $\Gamma(x, x')$. Thus for a fixed x, we have:

$$A_i(x, x', F) = \int_{\gamma \in \Gamma^m(x,x')} A_i^\gamma(x, x', F) d\mu(\gamma)$$

Note A'' is determined by x, x', T; but since T is determined by x, x'; A'' is determined by x, x'. Thus for fixed x', we may obtain a μ for any x.

□

F Proof of Theorem 3

Proof. Suppose the suppositions of the theorem. We may assume that $x' = 0$, $x \geq 0$, for otherwise we may use the transformation technique applied in theorem 2. If F is C^1, done. Otherwise suppose the domain of F can be partitioned into a set of convex polytopes with F a local linear classifier on each polytope.

We now turn to a useful lemma, but before we do, we give the following definitions. Suppose for some i, $y \in [x, x']$, we define a straight line path from one side of the hyperrectanblge $[x, x']$ to the other given by: $\gamma_i^{(y,i)}(t) = x'_i + (x_i - x'_i)t$, $0 \leq t \leq 1$, and $\gamma_j^{(y,i)}(t) = y_j$, for $i \neq j$, for $0 \leq t \leq 1$. We say that F is non-decreasing from x to x' in it's i^{th} component if, for all $y \in [x, x']$, $F * \gamma^{(y,i)}$ is non-decreasing in t.

Lemma 3. Let A satisfy linearity, completeness, sensitivity(b), and NDP. Suppose $F \in \mathcal{F}$ is Lipschitz continuous and non-decreasing from x to x' in its i^{th} component. Then $A_i(x, x', F) \geq 0$.

Proof. Since F is Lipschitz, there exists c such that $F + c^T y$ is non-decresing from x' to x with $c_i = 0$. Note that $\partial_i(F - F - c^T y) = 0$. Thus $A_i(x, x', F) = A_i(x, x', F - F - c^T y) + A_i(x, x', F + c^T y) = A_i(x, x', F + c^T y) \geq 0$. □

Observe that since F is a linear classifier inside any of the polytopes that partition the domain, $\frac{\partial F}{\partial x_i}$ is a plain in each polytope, with the plain's height equal to the coefficient of x_i for that linear classifier. Fix i and let $\{f_m\}$ be any sequence with $f_m : [0, x] \to \mathbb{R}^n$ and the following properties:

- f_m is C^1.
- $f_m \leq \frac{\partial F}{\partial x_i}$ where defined.
- $\lim f_m = \frac{\partial F}{\partial x_i}$ almost everywhere.
- There exists k such that $||f_m|| \leq k$ for all m.

That is, $\{f_m\}$ is a sequence of bounded C^1 under-approximations of $\frac{\partial F}{\partial x_i}$ with a limit of $\frac{\partial F}{\partial x_i}$.

Define $F_m := \int_0^{x_i} f_m(x_{-i}, t)dt$. For $j \neq i$, we have $\frac{\partial F_m}{\partial x_j} = \int_0^{x_i} \frac{\partial f}{\partial x_j}(x_{-i}, t)dt$ by Leibnitz integral rule. Thus $\frac{\partial F_m}{\partial x_j}$ exists, is continuous. So F_m is C^1. Since ∇F exists except on the polytope boundaries, and $\nabla F_m < \nabla F$ on the interior of each polytope, $F - F_m$ is non-decreasing from x to x' in its i^{th} component for each m. So $A_i(x, x', F - F_m) \geq 0$ and, $A_i(x, x', F) \geq A_i(x, x', F_m)$. We note that $\lim \nabla F_m$ exists for almost every γ (with respect to μ^x). Thus,

$$
\begin{aligned}
&A_i(x, x', F) \\
&\geq \lim A_i(x, F_m) \\
&= \lim \int_{\gamma \in \Gamma^m(x)} A_i^\gamma(x, F_m) d\mu^x(\gamma) \\
&= \lim \int_{\gamma \in \Gamma^m(x)} \int_0^1 f_m \frac{\partial \gamma_i}{\partial t} dt d\mu^x(\gamma) \\
&= \int_{\gamma \in \Gamma^m(x)} \int_0^1 \lim f_m \frac{\partial \gamma_i}{\partial t} dt d\mu^x(\gamma) \\
&= \int_{\gamma \in \Gamma^m(x)} \int_0^1 \frac{\partial F}{\partial \gamma_i} \frac{\partial \gamma_i}{\partial t} dt d\mu^x(\gamma)
\end{aligned}
$$

We move the limit inside the interior integral by the dominated convergence theorem. We can move the limit inside the interior integral because f_m is bounded, $\frac{\partial \gamma_i}{\partial t}$ is bounded using the constant velocity path parameterization, and the interior terms have a point-wise limit almost everywhere for almost every γ. To move the limit into the first integral, note that for particular values of c_i we can employ Lemma 3 to bound $A_i^\gamma(x, F_m + c_i y_i)$ above or below zero and $A_i^\gamma(x, c_i y_i) = c_i$, implying that $A_i^\gamma(x, F_m)$ is bounded for almost every γ. Using an over approximating sequence for $\{f_m\}$ instead of an under approximating sequence yields the same inequality in reverse.

□

G Proof of Theorem 4

First, we begin with the counterexamples. We will denote the integrated gradient method by IG. Consider $F(y_1, y_2) = \max(y_2 - y_1, y_1 - y_2)$. Let $\epsilon > 0$. Set $x' = (0, 0)$ and consider $x = (1, 1 + \frac{\epsilon}{2})$, $\bar{x} = (1, 1 - \frac{\epsilon}{2}$. Let $\gamma, \bar{\gamma}$ be the IG paths corresponding to $x, \bar{x}$, respectively.

First, note that $||x - \bar{x}|| = \epsilon$. We find that $\frac{\partial F}{\partial y_1} = 1$ if $y_1 > y_2$, and $\frac{\partial F}{\partial y_1} = -1$ if $y_1 < y_2$. So $\text{IG}_1(x, x', F) = (x_1 - x'_1)\int_0^1(-1)dt = 1$, while $\text{IG}_1(\bar{x}, x', F) = -1$. So $|I(x, x', F) - I(\bar{x}, x', F)| = 2$. Thus $I(x, x', F)$ is not Lipschitz continuous in x. Now we present the proof of the second claim:

Proof. Fix x' and let F be such that ∇F is Lipschitz continuous. Choose any $x, \bar{x} \in [a, b]$. We will denote the uniform-velocity paths for $x, \bar{x}$ by $\gamma, \bar{\gamma}$, respectively. Then,

$$
\begin{aligned}
&|\text{IG}_i(x, x', F) - \text{IG}_i(\bar{x}, x', F)| \\
=&|(x_i - x'_i)\int_0^1 \frac{\partial F}{\partial x_i}(\gamma(t))dt - (\bar{x}_i - x'_i)\int_0^1 \frac{\partial F}{\partial x_i}(\bar{\gamma}(t))dt| \\
=&|(x_i - \bar{x}_i)\int_0^1 \frac{\partial F}{\partial x_i}(\gamma(t))dt - (\bar{x}_i - x'_i)\int_0^1 [\frac{\partial F}{\partial x_i}(\bar{\gamma}(t)) - \frac{\partial F}{\partial x_i}(\gamma(t))]dt| \\
\leq&|x_i - \bar{x}_i|\int_0^1 |\frac{\partial F}{\partial x_i}(\gamma(t))|dt + |\bar{x}_i - x'_i|\int_0^1 |\frac{\partial F}{\partial x_i}(\bar{\gamma}(t)) - \frac{\partial F}{\partial x_i}(\gamma(t))|dt
\end{aligned}
$$

∇F is bounded, so $\int_0^1 |\frac{\partial F}{\partial x_i}(\gamma(t))|dt < C_1$, for some C_1. Since ∇F is Lipschitz continuous, $|\frac{\partial F}{\partial x_i}(\bar{\gamma}(t)) - \frac{\partial F}{\partial x_i}(\gamma(t))| \leq C_2||\gamma(t) - \bar{\gamma}(t)|| \leq C_2||x - \bar{x}||$ for some C_2. By the bounded domain, $|\bar{x}_i - x'_i| \leq ||b - a||$. Thus,

$$
\begin{aligned}
&|x_i - \bar{x}_i|\int_0^1 |\frac{\partial F}{\partial x_i}(\gamma(t))|dt + |\bar{x}_i - x'_i|\int_0^1 |\frac{\partial F}{\partial x_i}(\bar{\gamma}(t)) - \frac{\partial F}{\partial x_i}(\gamma(t))|dt \\
\leq&||x - \bar{x}|| * C_1 + ||b|| * C_2||x - \bar{x}||
\end{aligned}
$$

Thus $\text{IG}_i(x, x', F)$ is Lipschitz continuous. □

H IG Visualizations on Fashion MNIST

We apply the original IG with back image as baselines to the examples in Fashion MNIST dataset. The visualizations are show in Figure 5 (Middle). Green dots show positive IG while red dots show negative IG. It can be seen that almost all the attributes on the images are green, indicating that the model is recognizing/classifying the images correctly. Figure 5 (Right) shows the IG attributes computed with uniform random noise as baseline. It is quite interesting to note the model leverages some item features to do the classification. For example, IG is concentrated around the arch of sneakers and around two sides of the long skirts. Figure 6 visualizes the distribution of IG values with black images and uniform random images used as baselines respectively. It can be seen that when random baselines are used, the computed IG values are less extreme.

I Additional Experiments in Section 6.2

We redo the experiment of Section 6.2 but with another category, T-shirt/top. One thing worth mentioning is that we pick two representative categories: Sneaker and T-shirt/top, of which the natural testing accuracy is above and below the median accuracy respectively. It can be seen that after pruning the neurons with lowest ranked IG values, we can close the gap of accuracies between T-shirt/top and the median. (Compare purple and red curves in Figure 7 Left. The red curve starts above the purple curve. After pruning, purple curve rises above red curve). On the right side of Figure 7, we suppress the performance of T-shirt/top class by pruning top ranked neurons in terms of their corresponding IG values. The rising tip at the rightmost of the figure is due to the neurons which have the negative IG value. When they

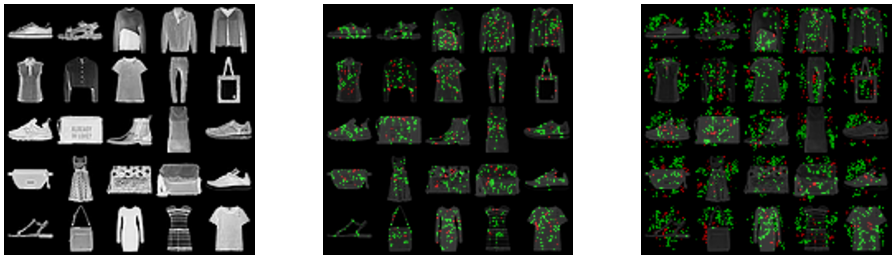

Figure 5: Left: Examples from the Fashion MNIST dataset. Middle: Visualization of Integrated Gradient (IG) on the examples with black image as baseline. Green dots show positive IG values and red dots show negative IG values. Right: Visualization of Integrated Gradient (IG) values on the examples with uniform random noise as baseline.

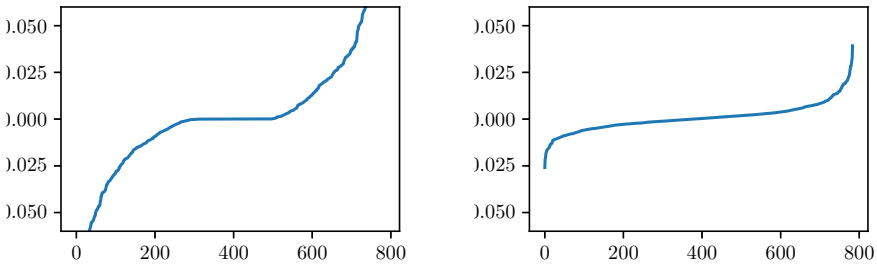

Figure 6: Distribution of the IG attributes (after sorting). X-axis is the index of the pixel and y-axis is the IG value. Left: black image is used as baselines. Right: uniform random noises are used as baselines.

are zeroed out, there exists a temporary overshoot since the output confidence can not be suppressed by the negative IG neurons.

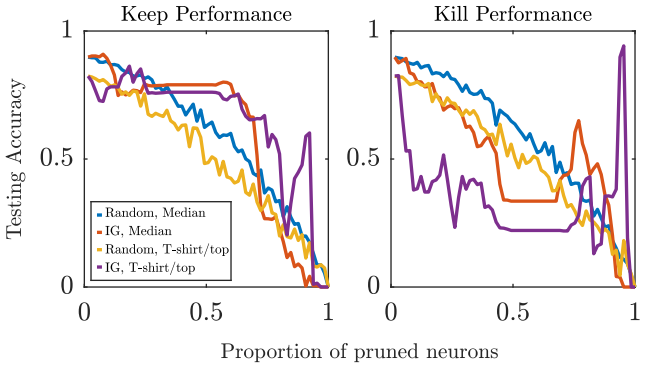

Figure 7: Performance of the model when neurons are pruned according to their IG values corresponding to T-shirt/top. "Random, Median", "IG, Median" report median accuracies among all classes and the neurons are pruned randomly and by their IG value respectively. "Random, T-shirt/top", "IG, T-shirt/top" report accuracy of class Sneaker only and the neurons are pruned randomly and by their IG value respectively. Left: Prune neurons by their IG values in ascending order. Right: Prune neurons by their IG values in descending order.

J Model Architecture and Training Parameters

Table 2 presents the architecture of the model used in the experiments.

Layer Type	Shape
Convolution + tanh	$5 \times 5 \times 5$
Max Pooling	2×2
Convolution + tanh	$5 \times 5 \times 10$
Max Pooling	2×2
Fully Connected + tanh	160
Fully Connected + tanh	64
Softmax	10

Table 2: Model Architecture for the Fashion MNIST dataset